ACS Medicinal Chemistry Letters

Letter

Novel copper complexes that inhibit the proteasome and trigger apoptosis in triple-negative breast cancer cells

Dong-Dong Li, Ernesto Yagüe, Lu-Yao Wang, Lin-Lin Dai, Zi-Bo Yang, Shuang Zhi, Na Zhang, Xiu-Mei Zhao, and Yun-Hui Hu

ACS Med. Chem. Lett., **Just Accepted Manuscript** • DOI: 10.1021/acsmedchemlett.9b00284 • Publication Date (Web): 25 Jul 2019

Novel copper complexes that inhibit the proteasome and trigger apoptosis in triple-negative breast cancer cells

Dong-Dong Li [1*], Ernesto Yagüe[3], Lu-Yao Wang[1], Lin-Lin Dai[1], Zi-Bo Yang[1], Shuang Zhi[1], Na Zhang[1], Xiu-Mei Zhao[1*], Yun-Hui Hu[2*]

[1]Tianjin Institute of Medical and Pharmaceutical Sciences, Tianjin 300020, China
[2]The Third Department of Breast Cancer, Tianjin Medical University Cancer Institute and Hospital, Tianjin 300060
[3]Cancer Research Center, Division of Cancer, Faculty of Medicine, Imperial College London, Hammersmith Hospital Campus, London W12 0NN, UK
*Corresponding authors:
Dong-Dong Li, Tianjin Institute of Medical and Pharmaceutical Sciences, E-mail address: lidongdong2010@163.com;
Xiu-Mei Zhao, Tianjin Institute of Medical and Pharmaceutical Sciences, E-mail address: zxmmlg@163.com;
Yun-Hui Hu, The Third Department of Breast Cancer, Tianjin Medical University Cancer Institute and Hospital, E-mail: yunhuihu200408@163.com.

KEYWORDS: *amino acid-polypyridine-copper complexes, proteasome inhibition, apoptosis induction,triple-negative breast cancer therapy*

ABSTRACT: Five innovative ternary copper(II) complexes [Cu(OH-PIP)(Phe)Cl](**1**), [Cu(OH-PIP)(Gly)(H_2O)]NO_3·2H_2O (**2**), [Cu(OH-PIP)(Ala)(Cl)]·H_2O (**3**), [Cu(OH-PIP)(Met)]PF_6·2H_2O (**4**), [Cu(OH-PIP)(Gln)(H_2O)](Cl)·3H_2O (**5**) have been synthesized and characterized by infrared spectroscopy, elemental analysis, and single crystal X-ray diffraction analysis. X-ray crystallography indicates that all Cu atoms are five-coordinated in a square-pyramidal configuration. The complexes have been screened for cytotoxicity against human breast cancer cell lines MCF-7, MDA-MB-231 and CAL-51. The best anticancer activity is obtained with triple-negative breast cancer CAL-51 and MDA-MB-231 cell lines, with IC_{50} values in the range of 0.082-0.69 μM. Importantly, the copper compounds were more effective than carboplatin at triggering cell death. Mechanistically, the complexes inhibit proteasomal chymotrypsin-like activity, and docking studies reveal their 20S proteasome binding sites. As a consequence, they cause the accumulation of ubiquitinated proteins, inhibit cell proliferation and induce apoptosis. In addition, these copper complexes decrease the stemness of triple-negative breast cancer cells, and have synergistic effects with CBP on TNBC cells, indicating their great potential as a novel therapy for triple-negative breast cancer.

The ubiquitin-proteasome system (UPS) plays an important role in multitude of cellular processes including cell cycle progression, apoptosis, angiogenesis, DNA damage and repair, drug resistance and differentiation [1]. The 20S proteasome is a high molecular weight protease complex with a proteolytic core containing β1, β2 and β5subunits, which are responsible for its caspase-like, trypsin-like and chymotrypsin-like (CT-like) activities, respectively. It is well established that inhibition of the β5 proteasomal subunit is primarily associated with apoptosis induction in tumor cells [2-4]. Proliferation and apoptosis pathways are tightly regulated in the cell by the UPS and alterations in the UPS may result in cellular transformation or other pathological conditions. As the proteasome is often found to be overactive in cancer cells making it more sensitive to proteasome inhibition than normal cells, the development of proteasome as novel anticancer drugs has been sought for some time [5].

Most proteasome inhibitors are short peptides that mimic protein substrates [6]. Bortezomib and carfilzomib, approved by the US Food and Drug Administration, have proven to be effective therapeutic agents for multiple myeloma and mantle cell lymphoma[7-12]. However, these drugs have not been successful in treating patients with solid cancers, probably due to poor *in vivo* stability, undesirable pharmacokinetic properties and unwanted toxicities arising from peptide backbones and electrophilic pharmacophores [13-17]. Thus, there is an urgent need to generate new molecules that can inhibit the proteasome utilizing a non-peptide scaffold which could overcome these drawbacks.

Metal-containing drugs have existed for decades and cisplatin, a platinum containing compound, is known as one of the most

effective antitumor drugs. Nowadays, the platinum drugs are still in the front line of metal-based cancer chemotherapy[18,19]. However, their negative side-effects and the risk of resistance remain a pressing matter in their clinical use. These issues drive the research and development of new metallotherapeutics, in many cases divergent from the platinum metals-based complexes [20]. Copper is biocompatible and less toxic than non-endogenous heavy metals. This makes it an interesting candidate for the treatment of cancers due to its bioavailability and the observation of increased copper levels in cancer tissue [21]. Therefore, copper complexes are regarded as one of the most promising alternatives to cisplatin as anticancer substances[22]. Copper complexes called Casiopeínas® have proved their significant anticancer activity both in preclinical *in vitro* and *in vivo* testing and two of them have entered Phase I clinical trials [23]. J. Zuo [24] *et al.* have reported two amino acid Schiff base-copper complexes which could inhibit the chymotrypsin-like activity of 20S proteasome, cause accumulation of proteasome target proteins bax and IκB-α, and induce growth inhibition and apoptosis in MDA-MB-231, MCF-7 and PC-3 tumor cells. Z.Y. Zhang [25] *et al.* have reported a L-Ornithine Schiff base-copper complex with proteasome-inhibitory activities and induction of apoptosis in MDA-MB-231 and LNCaP cancer cells.

Previously, we have reported some polypyridine-copper complexes as antitumor agents [26-28]. These copper complexes are toxic to HeLa and MCF-7 cells, with IC_{50} values in the range of 6.70-16.58 μM, inducing apoptosis in human cancer cells and inhibiting tumor cell growth, although their molecular mechanisms remain to be established. In order to improve the targeting and solubility of this type of complex we introduced an amino acid and generated five novel amino-polypyridine-copper complexes. We found that they inhibit the proteasomal chymotrypsin-like activity, cause accumulation of ubiquitinated proteins, and induce growth inhibition and apoptosis in dose-dependent manners. They also decrease the stemness of triple negative breast cancer (TNBC) cells, indicating their great potential as a novel therapy for triple-negative breast cancer.

The synthesis and characterizations of complexes **1-5** were described in supporting information. They have been structurally characterized by X-ray crystallography (Figure 1). The crystallographic data and structure refinement parameters for the complexes **1-5** were seen in Tables 1S and 2S.

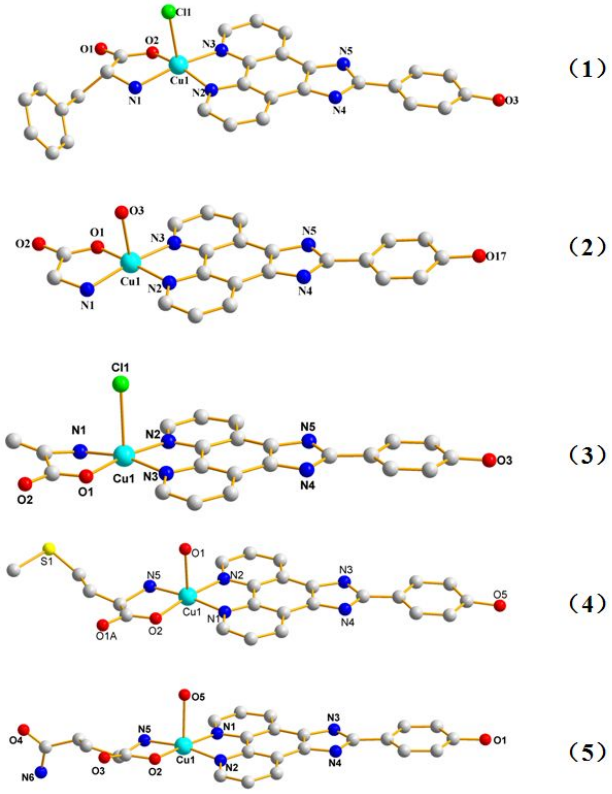

Figure 1 Molecular structures of complexes **1-5**, dissociative small molecules and non-essential H-atoms.

Complexes **1-5** were evaluated for their antiproliferative activity against human breast tumor CAL-51, MDA-MB-231 and MCF-7 cells by using an MTT assay, and comparing their cytotoxicity to carboplatin (CBP). IC_{50} values for complexes **1-5** were lower than those of the free ligand and copper salt in all of the tested cells, which suggests that the coordinated copper(II) ion plays a major role in mediating the potency of the complexes (Table 1). The complexes **1-5** had lower IC_{50} values than CBP against the three breast cancer cells, indicating that these novel complexes have stronger toxicity than carboplatin, a platinum compound commonly used in the clinic. The complexes **1-5** had extremely low IC_{50} levels on CAL-51 cells, with the order of the cytotoxicity being **3** > **5** > **2** > **1** >**4**, indicating that the configuration of the amino acid affects the activity of the complexes. As complexes **3** (IC_{50} = 0.08 μM) and **5** (IC_{50} = 0.27 μM) were the most potent, their biological activity on TNBC CAL-51 and MDA-MB-231 cells was evaluated further.

Table 1 The anti-proliferative effects of complexes **1-5** against various breast cancer cells

Complex	IC_{50} (μM)		
	CAL-51	MDA-MB-231	MCF-7
1	0.52±0.02	18.89±1.23	30.88±2.56
2	0.37±0.04	10.98±0.95	25.59±2.10
3	0.08±0.004	8.35±0.55	17.08±1.64
4	0.69±0.04	4.92±0.36	18.99±1.54
5	0.27±0.02	9.33±0.84	20.32±2.01
Copper salt	＞100	＞100	＞100
OH-PIP	18.51±1.5	22.84±2.1	68.08±3.2
Carboplatin	1.05±0.1	15.02±1.4	36.65±2.5

To determine whether the complexes **3** and **5** have synergistic effects with CBP on TNBC cells, MDA-MB-231 and CAL-51 cells were treated with 3 μM CBP and different concentrations of either complex **3** or **5** for 48 h, and the proliferation was assessed by MTT assay. MDA-MB-231 cells treated with 0.39-25.0 μM **3** and 0.19-12.5 μM **5** showed CI values in the range 0.50-0.93 and 0.03-0.92, respectively. Similarly, CAL-51 cells treated with 0.19-6.25 μM **3** and 0.19-6.25 μM **5** showed CI values in the range of 0.37-0.96 and 0.43-0.86, respectively. In all cases CI values were lower than 1.0 (Tables 3S and 4S), indicating synergistic effects between the novel copper compounds and CBP on breast cancer cells.

To investigate whether the growth-inhibitory activity of the complexes **1-5** was associated with their ability to inhibit the proteasome activity, purified human 20S proteasome was treated with a range of compound concentrations for 2 h at 37 °C in the presence of fluorogenic Suc-LLVY-AMC, a specific substrate for the CT-like activity. The results indicate that these copper complexes did inhibit the proteasomal CT-like activity in a dose-dependent manner and more efficiently than either the free ligand or copper salt (Figure 2). Thus, complexes **1-5** target the 20S proteasomal catalytic β5 subunit.

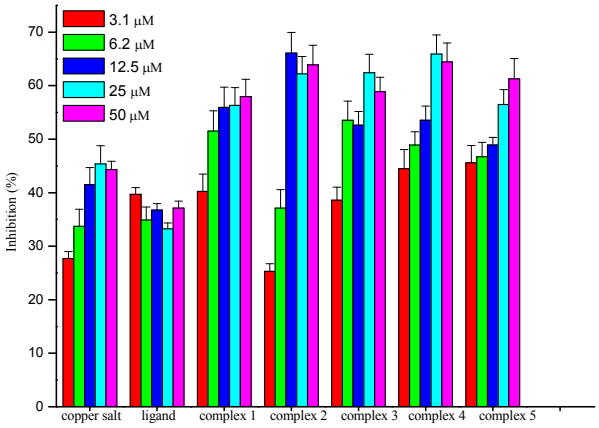

Figure 2 The copper complexes inhibit proteasomal CT-like activity *in vitro*. Purified 20S proteasome was incubated in the presence of increasing concentration of copper salt, ligand and copper complexes **1-5** and the CT-like activity measured by the production of fluorescent AMC groups from Suc-LLVY-AMC substrate. Data represent the average ± SD of three independent experiments.

In order to ascertain that proteasome inhibition by the copper complexes is associated with apoptosis induction, cellular morphological changes were monitored in MDA-MB-231 and CAL-51 cells after 24 h treatment. Cells treated with complexes **3** and **5** at a concentration double of their IC_{50} appeared with characteristic dose-dependent apoptotic blebbing (Figures 1S). These results suggest that complexes **3** and **5** have the ability to inhibit the proteasome and induce apoptosis in a concentration-dependent manner in MDA-MB-231 and CAL-51 cells.

To elucidate the mechanism by which copper complexes cause cell death in human tumor cells, we performed apoptotic assays by Annexin V-propidium iodide staining in cells after 24 h treatment with the complexes at 1 × and 2 × their IC_{50}. In MDA-MB-231 cells, complex **3** at 8.35 and 16.70 μM triggered cell death in a dose-dependent manner, with total apoptotic values of 7.5 % and 56.9 %, respectively. In a similar fashion, apoptotic values of complex **5** at 9.33 and 18.66 μM were 56.5 % and 74.5 %, respectively. Importantly, most of the cell death reported was due to cells in early apoptosis (Figure 3). CAL-51 cells responded in the same way: complex **3** at 0.082 and 0.16 μM triggered cell death in a dose-dependent manner, with total apoptotic values of 8.6 % and 15.5 %, respectively, whereas the apoptotic values after treatment with complex **5** at 0.27 and 0.54 μM were 10.5 % and 14.4 %, respectively (Figure 4). Although **3** and **5** induced apoptosis more efficiently in MDA-MB-231 than in CAL-51 cells, overall these results indicate that both compounds induce apoptosis in a dose-dependent manner in TNBC cells.

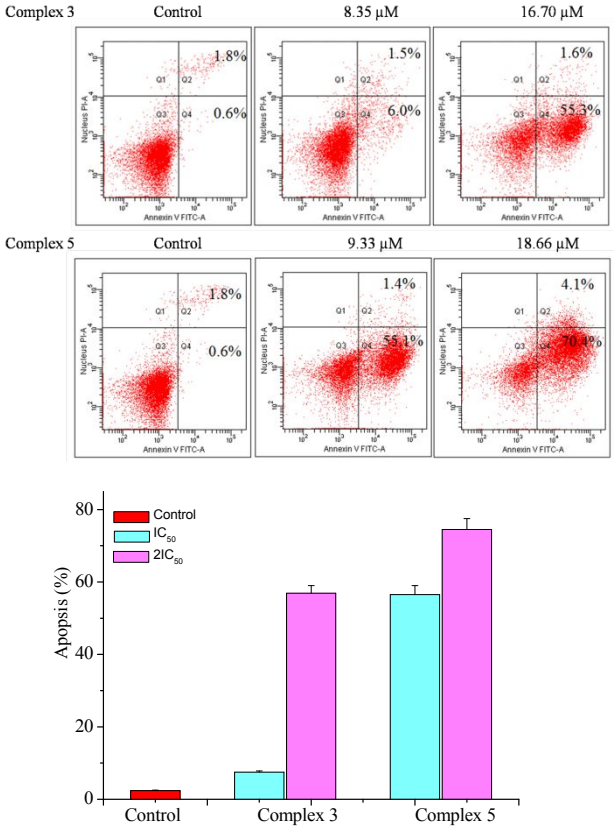

Figure 3 The copper complexes induce apoptosis in TNBC MDA-MB-231 cells. Cells were treated with the copper complexes at 1× and 2 × IC_{50} concentrations for 24 h and apoptosis detected by flow cytometry using annexin V (x axis)– propidium iodide (y axis) staining. Early apoptotic cells (annexin V-positive, propidium iodide-negative) appear in the lower right quadrant and late apoptotic cells (positive for both markers) in the upper right quadrant. Percentage of cells in apoptotic quadrants is shown. Cytometry plots are representative three independent experiments. Histogram indicates average apoptosis (both early and late) ± SD from three independent experiments.

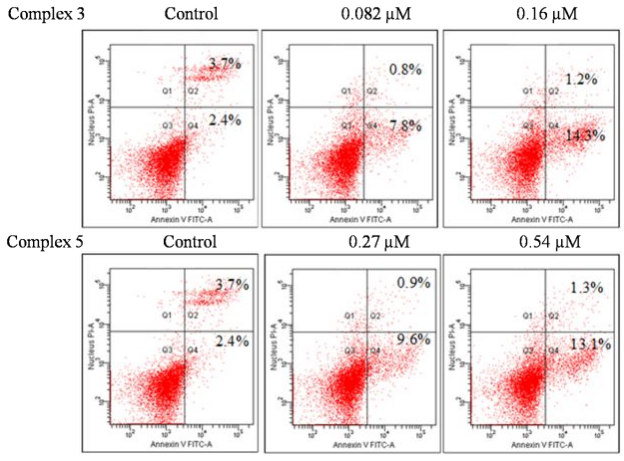

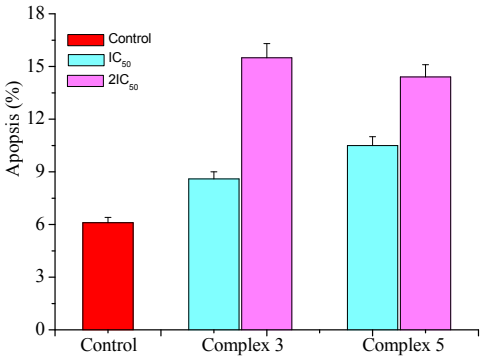

Figure 4 The copper complexes induce apoptosis in TNBC CAL-51 cells. Cells were treated with the copper complexes at 1 × and 2 × IC_{50} concentrations for 24 h and apoptosis detected by flow cytometry using annexin V (x axis) –propidium iodide (y axis) staining. Early apoptotic cells (annexin V-positive, propidium iodide-negative) appear in the lower right quadrant and late apoptotic cells (positive for both markers) in the upper right quadrant. Percentage of cells in apoptotic quadrants is shown. Cytometry plots are representative three independent experiments. Histogram indicates average apoptosis (both early and late) ± SD from three independent experiments.

Key regulators of the apoptotic pathway include Bax, Bcl-2 and Caspase family proteins. When Bax expression is high, cells proceed to apoptosis, whereas when Bcl-2 is produced in excess, cells are protected from apoptosis [29]. In order to validate the functional results shown above, and to gain insights into the molecular mechanisms of cell death triggered by the copper complexes, we used western blots to detect Bax, Bcl-2 and caspase-3 protein expression in MDA-MB-231 and CAL-51 cells treated with **3** and **5** at the IC_{50} and 2 × IC_{50} for 24 h. Levels of Bax protein increased, while Bcl-2 and caspase-3 protein expression levels were downregulated, upon treatment with the copper complexes (Figure 5). Furthermore, the PARP cleavage fragment p89 appeared after 24 h treatment, indicating that the cancer cells were undergoing apoptosis. In addition, and consistent with the inhibition of proteasomal inhibiton under cell-free conditions, increased level of ubiquitinated proteins were also detected in a dose-dependent fashion upon copper complexes treatment. These cellular data further indicate that the complexes inhibit proteasome activity and induce apoptosis.

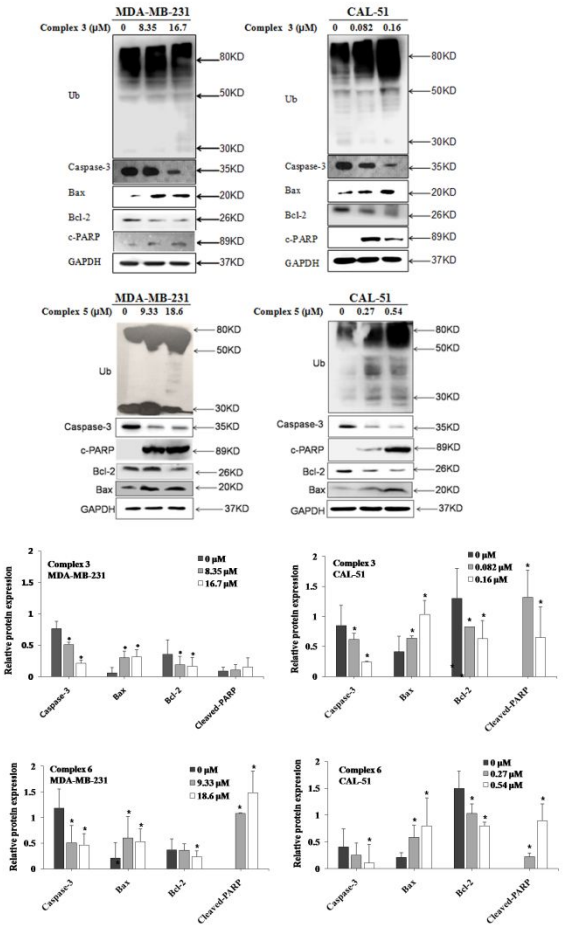

Figure 5 Complexes **3** and **5** induce accumulation of ubiquitinated proteins and apoptosis. Breast cancer MDA-MB-231 and CAL-51 cells were treated with **3** and **5** at 1 × and 2 × IC_{50} concentrations for 24 h and ubiquitinated proteins, Caspase-3, PARP, Bcl-2 and Bax. proteins detected by western blotting. Housekeeping GAPDH levels were used to confirm equal protein loading. Arrow indicates molecular mass in kDa. Band intensity was quantified using Image J and shown as the average ± SD (n=3), *P＜0.05.

Cancer stem cells (CSCs), a subpopulation of tumor cells possessing the extensive self-renewal capability necessary to successfully colonize distant organs, relate to highly aggressive TNBC [30]. The $CD44^+/CD24^-$ breast cancer cell subpopulation has a strong tumor forming ability and these markers are considered one of the best in the field to determine breast CSC [31-33]. In the treatment of breast cancer, the elimination of breast cancer stem cells is the key to completely cure the disease. To determine whether **3** and **5** have the capacity to modulate stem cell phenotypes, we determined the extent of $CD44^+/CD24^-$ population by flow cytometry. Indeed, MDA-MB-231 cells showed a dose-dependent decreases in $CD44^+/CD24^-$ stem cell population of 12.3 % and 13.4 % when treated with 16.7 μM complex **3** and 18.66 μM complex **5,** respectively (Figure 6 and Table 5S).

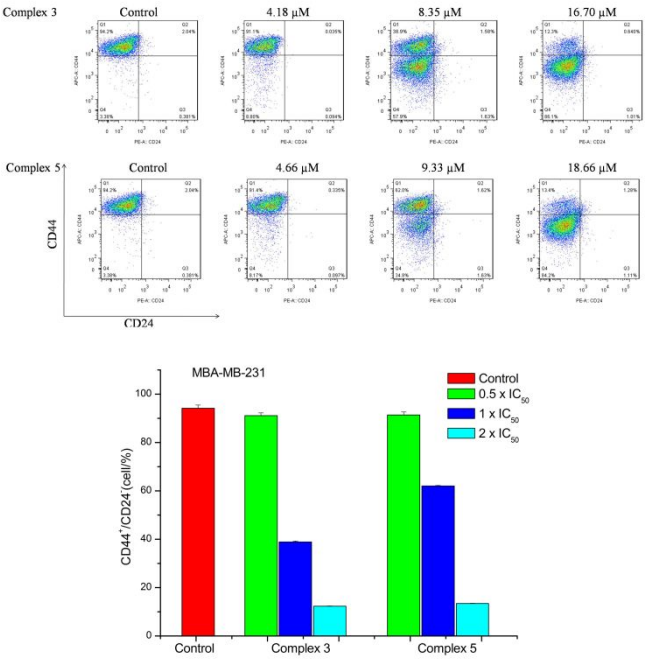

Figure 6 Complexes **3** and **5** decrease stem cell markers in MDA-MB-231 cells. Breast cancer MDA-MB-231 cells were treated with **3** and **5** at 0.5 ×, 1 × and 2 × IC_{50} concentrations for 24 h and the percentage of the $CD44^+/CD24^-$ cell subpopulation was determined by flow cytometry. Histogram indicates the average percentage of the $CD44^+/CD24^-$ cell subpopulation from three independent experiments.

As ALDH has also been identified as a CSC marker in different type of cancers, and represents the CSC subpopulation better than $CD44^+/CD24^-$ in CAL-51 cells [34], we also tested ALDH activity by ALDEFLUOR assay in both cell lines. Both complexes **3** and **5** reduced the percentage of ALDH-positive cells in a dose-dependent manner. In MDA-MB-231 cells, that show a 22.7% ALDH-positive cells, complex **3** treatment at 16.7 μM reduced them to 0.72 %, whereas treatment with **5** at 18.6 μM reduced them to 1.02 % (Figure 7). Similarly, CAL-51 cells, with 45.5 % ALDH-positive cells, when treated with complex **3** had a reduction in the percentage of ALDH-positive cells to 8.25 % and with complex **5** to 5.50 % (Figure 8 and Table 6S).

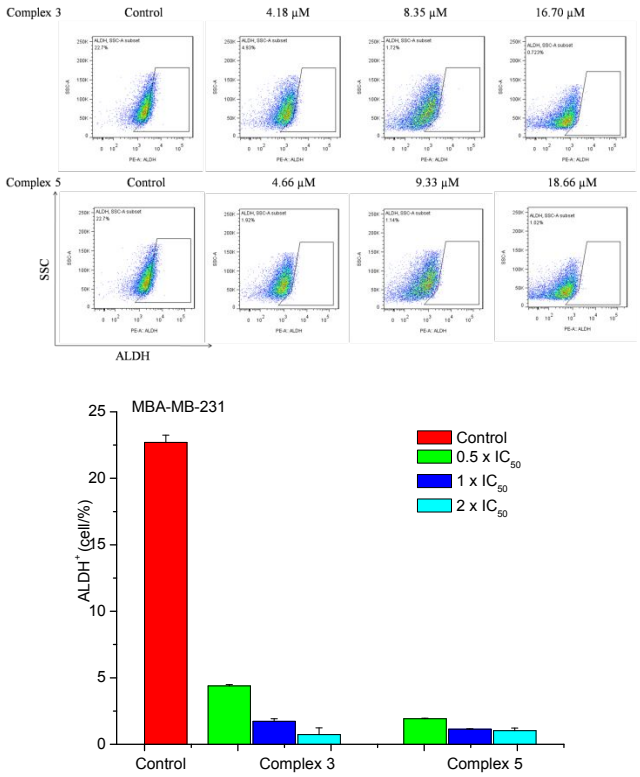

Figure 7 Complexes **3** and **5** decrease stem cell marker ALDH in MDA-MB-231 cells. Breast cancer MDA-MB-231 cells were treated with **3** and **5** at 0.5 ×, 1 × and 2 × IC_{50} concentrations for 24 h and the percentage of $ALDH^+$ cells determined by flow cytometry. In order to better visualize $ALDH^+$ cells, two-dimensional plots were obtained. SSC, side scatter channel. Histogram indicates the average percentage of the $ALDH^+$ cell subpopulation from three independent experiments.

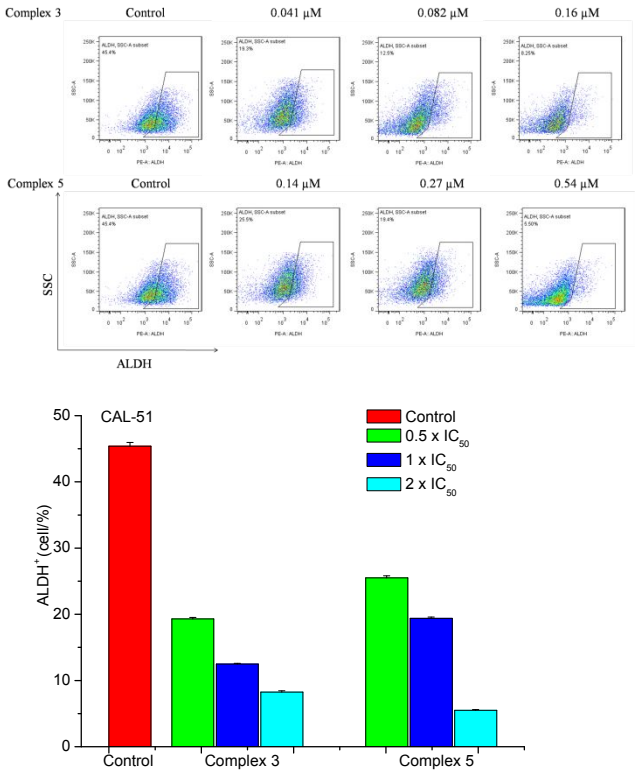

Figure 8 Complexes **3** and **5** decrease stem cell marker ALDH in CAL-51 cells. Breast cancer CAL-51 cells were treated with **3** and **5** at 0.5 ×, 1 × and 2 × IC_{50} concentrations for 24 h and the percentage of $ALDH^+$ cells determined by flow cytometry. In order to better visualize $ALDH^+$ cells, two-dimensional plots were obtained. SSC, side scatter channel. Histogram indicates the average percentage of the $ALDH^+$ cell subpopulation from three independent experiments.

Although CSC marker studies are informative, tumorsphere assays were carried out to investigate whether **3** and **5** did affect tumor forming characteristics *in vitro* and how they compared to CBP. Seen in Figure 2S, compared with control, Both TNBC cell lines produced robust tumorspheres that decreased in size after CBP treatment. However, **3** and **5** completely disaggregated the spheres and, at the highest dose, led to their depletion. Thus, both **3** and **5** decrease the stemness of TNBC cells.

The docking analysis provided new insights on a possible mechanism of proteasome inhibition. The molecular modeling results may account for the data observed in the purified proteasome studies. As shown in Figure 9, in addition to form hydrophobic interaction with the hydrophobic pocket composed of residues Ala-50, Ala-49, Ala-46, Met-45, Ala-31, Ala-20, Ala-22 and Ala-27, complex **1** formed hydrogen bonding through hydroxyl interaction with residue Ala-93, and formed hydrogen bonding through imidazole-NH with residue Gly-94, and formed hydrogen bonding through amino acid with residue Gly-47 and Ala-49; complex **2** formed hydrogen bonding through hydroxyl interaction with residue Lys-32, and formed hydrogen bonding through imidazole with residue Ala-49 and Thr-1, and formed hydrogen bonding through amino acid with residue Gly-23; complex **3** formed hydrogen bonding through amino acid with residue Thr-1, and formed a coordination bond between copper atom and residue Gly-47; complex **4** formed hydrogen bonding through imidazole-NH with residue Thr-1, and formed hydrogen bonding through amino acid with residue Lys-23, and formed hydrogen bonding through oxygen atom with residue Gln-53; complex **5** formed hydrogen bonding through amino acid with residues Thr-1 and Ser-129, and formed a coordination bond between copper atom and residue Gly-47. The minimum relative binding energy values were -7.51, -7.82, -6.51, -6.49 and -6.04 kcal/mol for **1-5**, respectively, indicating the interaction between the copper complexes and 20S proteasome.

Complex 1

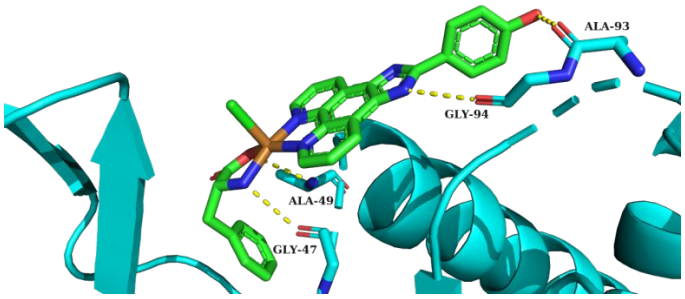

Complex 2

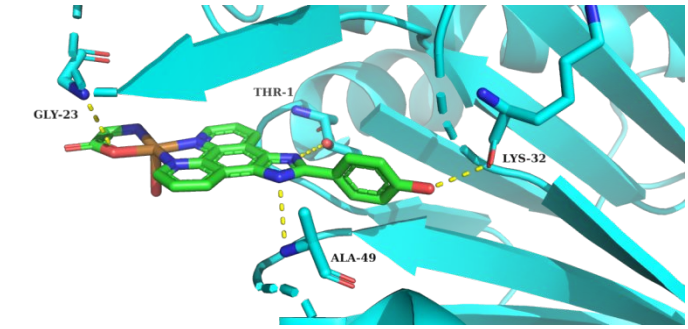

Complex 3

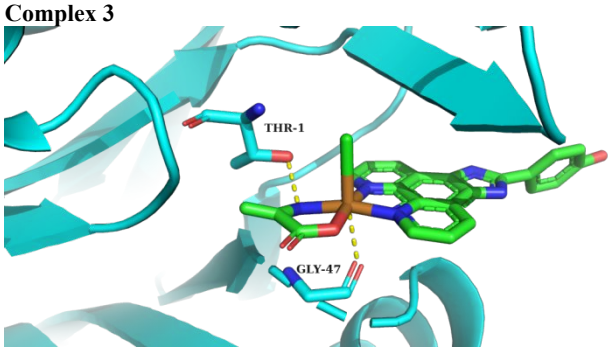

Complex 4

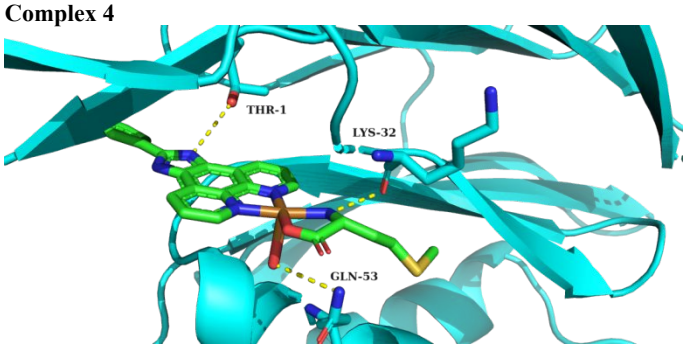

Complex 5

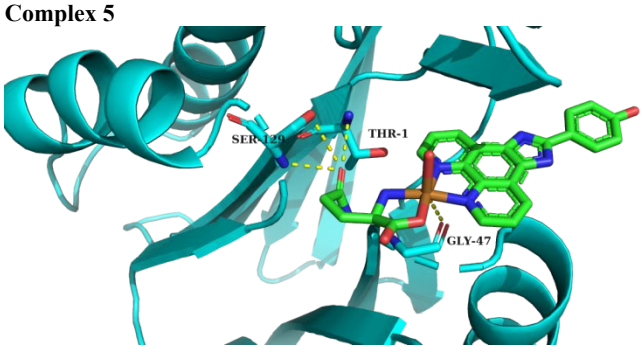

Figure 9 Schematic representation of the proposed binding modes for complexes **1-5** with proteasome (PDB ID:3MG6). Only amino acids located within 4 Å of the bound ligand are displayed and labeled. Key H-bonds between the complexes and the protein are shown as dashed yellow lines.

ASSOCIATED CONTENT

Supporting Information

Crystallographic data and structure refinement parameters, selected bond lengths (Å) and angles (º) for the complexes **1-5**. The CI values of combination of **3** or **5** and CBP for MDA-MB-231 and CAL-51 cells. The effect of **3** and **5** on $CD44^{+}/CD24^{-}$ phenotype cell subsets in MDA-MB-231 was detected by Flow cytometry. The effect of the **3** and **5** on the ratio of ALDH1+ cell population in MDA-MB-231 and CAL-51 was detected by Flow cytometry. **3** and **5** abolish tumor forming capacity of TNBC cells *in vitro*.

AUTHOR INFORMATION

Corresponding Author

*Dong-Dong Li, Tianjin Institute of Medical and Pharmaceutical Sciences, E-mail address: lidongdong2010@163.com;

*Xiu-Mei Zhao, Tianjin Institute of Medical and Pharmaceutical Sciences, E-mail address: zxmmlg@163.com;

*Yun-Hui Hu, The Third Department of Breast Cancer, Tianjin Medical University Cancer Institute and Hospital, E-mail: yunhuihu200408@163.com.

Author Contributions

The manuscript was written through contributions of all authors

Funding Sources

This work was supported by the National Natural Science Foundation of China (21501134).

Abbreviations

MCF-7	Human breast cancer cell line
MDA-MB-231	Human breast cancer cell line
CAL-51	Human breast cancer cell line
TNBC	triple-negative breast cancer
CBP	Carboplatin
CSCs	Cancer stem cells

REFERENCES

1. Soave, C. L.; Guerin, T.; Liu, J. B.; Dou, Q. P. Targeting the ubiquitin-proteasome system for cancer treatment: discovering novel inhibitors from nature and drug repurposing. *Cancer and Metastasis Reviews* **2017**, *36*, 717-736.
2. Manasanch, E. E.; Orlowski, R. Z. Proteasome inhibitors in cancer therapy. *Nature Reviews Clinical Oncology* **2017**, *14*, 417-433.
3. Lopes, U. G.; Erhardt, P.; Yao, R.; Copper, G. M. p53-dependent induction of apoptosis by proteasome inhibitors. *J. Biol. Chem.* **1997**, *272*, 12893-12896.

4. Daniel, K. G.; Gupta, P.; Harbach, R. H.; Guida, W. C.; Dou, Q. P. *Biochem. Pharmacol*. **2004**, *67*, 1139-1151.

5. Landis-Piwowar, K. R.; Milacic, V.; Chen, D.; Yang, H. J.; Zhao, Y. F.; Chan, T. H.; Yan, B.; Dou, Q. P. Organic copper complexes as a new class of proteasome inhibitors and apoptosis inducers in human cancer cells. *Drug Resistance Updates* **2006**, *9*, 263-273.

6. Kisselev, A. F.; van der Linden, W. A.; Overkleeft, H. S. Proteasome inhibitors: an expanding army attacking a unique target. *Chem. Biol.* **2012**, *19*, 99-115.

7. Chao, A.; Wang, T. H. Molecular mechanisms for synergistic effect of proteasome inhibitors with platinum-based therapy in solid tumors. *Taiwanese Journal of Obstetrics and Gynecology* **2016**, *55*, 3-8.

8. Jakubowiak, A. J. Evolution of carfilzomib dose and schedule in patients with multiple myeloma: a historical overview. *Cancer treatment reviews* **2014**, *40*, 781-790.

9. Ji, E. P.; Miller, Z.; Jun, Y.; Lee, W.; Kim, K. B. *Translational Research* **2018**, *198*, 1-16.

10. Mittenberg, A. G.; Kuzyk, V. O.; Shabelnikov, S. V.; Gorbach, D. P. Combined treatment of human multiple myeloma cells with bortezomib and doxorubicin alters the interactome of 20S proteasomes. *Cell Cycle* **2018,** *17*, 1745-1756.

11. Baker, A. F.; Hanke, N. T.; Sands, B. J.; Carbajal, L.; Anderl, J. L.; Garland, L. L. Carfilzomib demonstrates broad anti-tumor activity in pre-clinical non-small cell and small cell lung cancer models. *J. Exp. Clin. Cancer Res*. **2014**, *33*, 111.

12. Mehta, A.; Zhang, L.; Boufraqech, M.; Zhang, Y.; Patel, D.; Shen, M.; Kebebew, E. Carfilzomib is an effective anticancer agent in anaplastic thyroid cancer. *Endocrine-related cancer* **2015**, *22*, 319-329.

13. Chen, D.; Frezza, M.; Schmitt, S.; Kanwar, J.; Dou, Q. P. Bortezomib as the first proteasome inhibitor anticancer drug: current status and future perspectives. *Curr Cancer Drug Targets* **2011**, *11*, 239-253.

14. Siegel, D. S.; Martin, T.; Wang, M.; Vij, R.; Jakubowiak, A. J.; Lonial, S.; Trudel, S.; Kukreti, V.; Bahlis, N.; Alsina, M.; Chanan-Khan, A.; Buadi, F.; Reu, F. J.; Somlo, G.; Zonder, J.; Song, K.; Stewart, A. K.; Stadtmauer, E.; Kunkel, L.; Wear, S.; Wong, A. F.; Orlowski, R. Z.; Jagannath, S. A phase 2 study of single-agent carfilzomib (PX-171-003-A1) in patients with relapsed and refractory multiple myeloma. *Blood* **2012**, *120*, 2817-2825.

15. Yang, J.; Wang, Z.; Fang, Y.; Jiang, J.; Zhao, F.; Wong, H.; Bennett, M. K.; Molineaux, C. J.; Kirk, C. J. Pharmacokinetics, pharmacodynamics, metabolism, distribution, and excretion of carfilzomib in rats. *Drug Metab Dispos*, **2011**, *39*, 1873-1882.

16. Papadopoulos, K. P.; Burris, H. A.; Gordon, M.; Lee, P.; Sausville, E. A.; Rosen, P. J.; Patnaik, A.; Cutler, R. E.; Wang, Jr. Z.; Lee, S.; Jones, S. F.; Infante, J. R. A phase I/II study of carfilzomib 2–10-min infusion in patients with advanced solid tumors. *Cancer Chemother Pharmacol* **2013**, *72*, 861-868.

17. Wang, Z.; Yang, J.; Kirk, C.; Fang, Y.; Alsina, M.; Badros, A.; Papadopoulos, K.; Wong, A.; Woo, T.; Bomba, D.; Li, J.; Infante, J. R. Clinical pharmacokinetics, metabolism, and drug-drug interaction of carfilzomib. *Drug Metab Dispos* **2013**, *41*, 230-237.

18. Arnesano, F.; Natile; G. Mechanistic insight into the cellular uptake and processing of cisplatin 30 years after its approval by FDA. Coord. *Chem. Rev*. **2009**, *253*, 2070-2081.

19. Boulikas, T.; Pantos, A.; Bellis, E.; Christofis, P. Designing platinum compounds in cancer: structures and mechanisms. *Cancer* Ther. **2007**, *5*, 537-583.

20. Bruijnincx, P. C.; Sadler, P. J. New trends for metal complexes with anticancer activity. *Curr. Opin. Chem. Biol.* **2008**, *12*, 197-206.

21. Santini, C.; Pellei, M.; Gandin, V.; Porchia, M.; Tisato, F.; Marzano, C. New trends for metal complexes with anticancer activity. *Chem. Rev.* **2014**, *114*, 815-862.

22. Tabti, R.; Tounsi, N.; Gaiddon, C.; Bentouhami, E.; Désaubry, L. Progress in Copper Complexes as Anticancer Agents. *Medicinal chemistry* **2017**, *7*, 875-879.

23. Galindo-Murillo, R.; Garcia-Ramos, J. C.; Ruiz-Azuara, L.; Cheatham, T. E.; Cortes-Guzman, F. Intercalation processes of copper
complexes in DNA.*Nucleic Acids Res.* **2015**, *43*, 5364-5376.

24. Zuo, J.; Bi, C. F.; Fan, Y. H.; Buac, D.; Nardon, C.; Daniel, K. G.; Dou, Q. P. Cellular and computational studies of proteasome inhibition and apoptosis induction in human cancer cells by amino acid Schiff base–copper complexes. *Journal of Inorganic Biochemistry* **2013**, *118*, 83-93.

25. Zhang, Z. Y.; Bi, C. F.; Fan, Y. H.; Zhang, N.; Deshmukh, R.; Yan, X. C.; Lv, X. W.; Zhang, P. F.; Zhang, X.; Dou, Q. P. L-Ornithine Schiff base–copper and –cadmium complexes as new proteasome inhibitors and apoptosis inducers in human cancer cells. *J. Biol. Inorg. Chem*. **2015**, *20*, 109-121.

26. Li, D. D.; Tian, J. L.; Gu, W.; Liu, X.; Zeng, H. H.; Yan, S. P. DNA binding, oxidative DNA cleavage, cytotoxicity, and apoptosis-inducing activity of copper(II) complexes with 1,4-tpbd (*N,N,N′,N′*-tetrakis(2-yridylmethyl)benzene-1,4-diamine) ligand, *Journal of Inorganic Biochemistry* **2011**, *105*, 894-901.

27. Li, D. D.; Zhang, N.; Dai, L. L.; Yang, Z. B.; Tao, Z. W. Synthesis, DNA binding, nuclease activity and cytotoxic studies of a wheel - shaped octanuclear copper (II) complex based on 1,

2, 4 - triazole. *Applied Organometallic Chemistry* **2016**, *30*, 346-353.

28. Li, D. D.; Huang, F. P.; Chen, G. J.; Gao, C. Y.; Tian, J. L.; Gu, W.; Liu, X.; Yan, S. P. Four new copper (II) complexes with 1, 3-tpbd ligand: Synthesis, crystal structures, magnetism, oxidative and hydrolytic cleavage of pBR322 DNA. *Journal of Inorganic Biochemistry* **2010**, *104*, 431-441.
29. Cheah, P. L.; Looi, L. M. p53: an overview of over two decades of study. *Malays. J. Pathol.* **2001**, *23*, 9-16.
30. Clevers, H. The cancer stem cell: premises, promises and challenges. *Nat. Med.* **2011**, *17*, 313-319.
31. Wang, Z.; Kong, J.; Wu, Y.; Zhang, J.; Wang, T.; Li, N.; Fan, J.; Wang, H.; Zhang, J.; Ling, R. PRMT5 determines the sensitivity to chemotherapeutics by governing stemness in breast cancer. *Breast Cancer Res Treat* **2018**, *168*, 531-542.
32. Zhou, Z.; Li, M.; Zhang, L.; Zhao, H.; Sahin, O.; Chen, J.; Zhao, J. J.; Zhou, S. Y.; Yu, D. Oncogenic Kinase–Induced PKM2 Tyrosine 105 Phosphorylation Converts Nononcogenic PKM2 to a Tumor Promoter and Induces Cancer Stem–like Cells. *Cancer Res.* **2018**, *78*, 2248-2261.
33. Suman, S.; Das, T. P.; Damodaran, C. Silencing NOTCH signaling causes growth arrest in both breast cancer stem cells and breast cancer cells. *British Journal of Cancer* 2013, 109, 2587-2596.
34. Asaduzzaman, M.; Constantinou, S.; Min, H.; Gallon, J.; Lin, M. L.; Singh, P.; Raguz, S.; Ali, S.; Shousha, S.; Coombes, R. C.; Lam, E. W.; Hu, Y.; Yague, E. Tumour suppressor EP300, a modulator of paclitaxel resistance and stemness, is downregulated in metaplastic breast cancer. *Breast Cancer Res Treat* **2017**, *163*, 461-474.

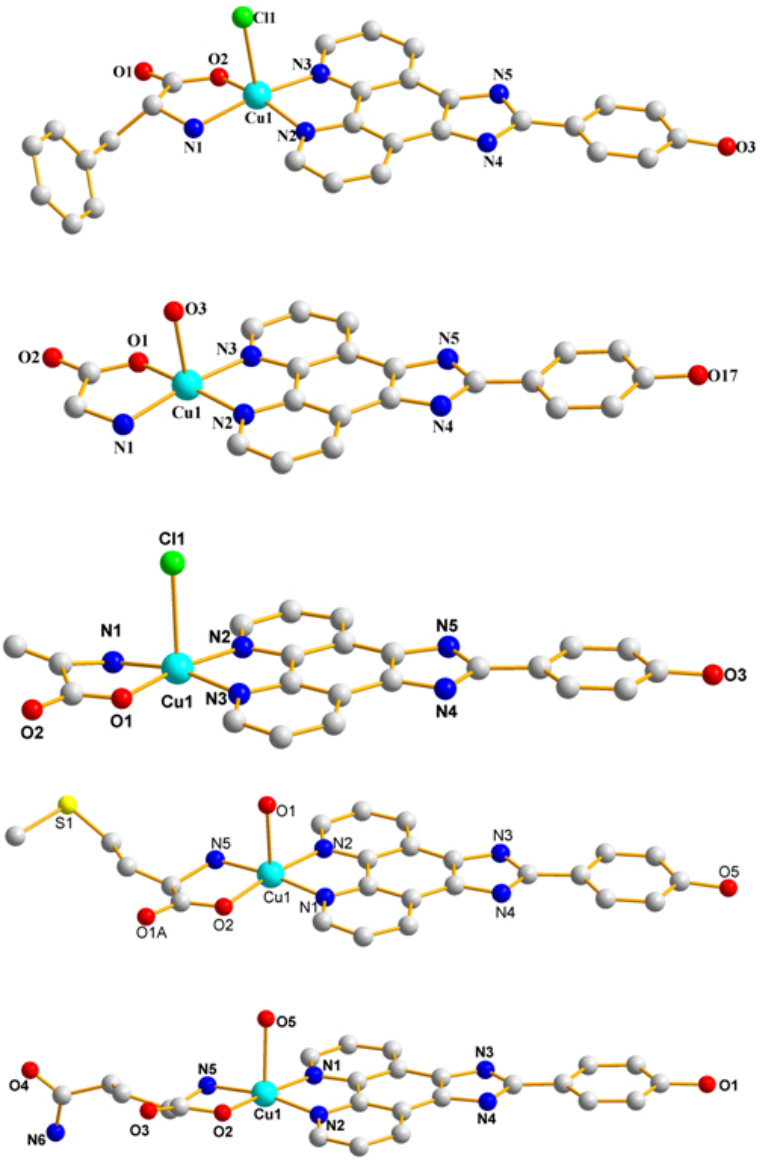

Molecular structures of complexes 1-5, dissociative small molecules and non-essential H-atoms.

218x280mm (72 x 72 DPI)

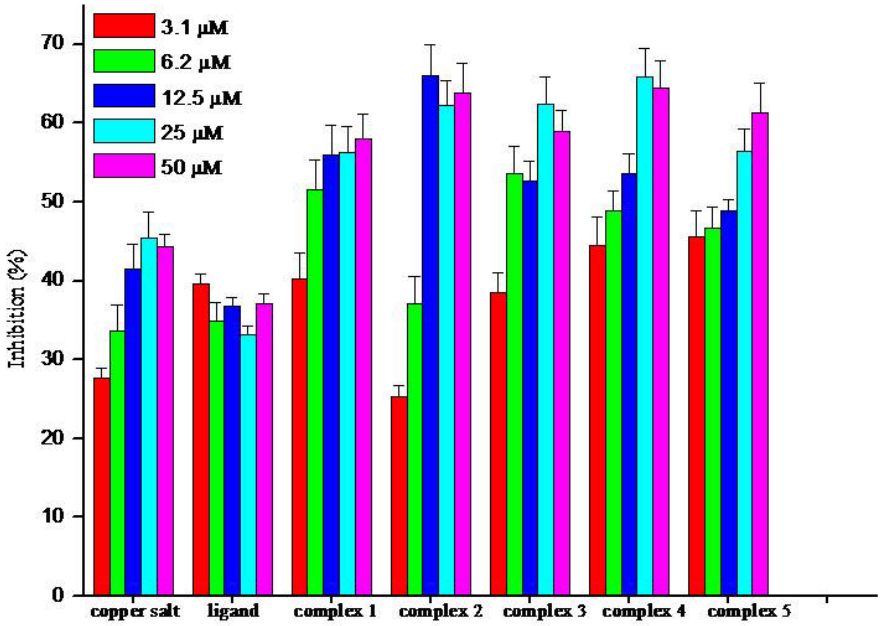

The copper complexes inhibit proteasomal CT-like activity in vitro. Purified 20S proteasome was incubated in the presence of increasing concentration of copper salt, ligand and copper complexes 1-5 and the CT-like activity measured by the production of fluorescent AMC groups from Suc-LLVY-AMC substrate. Data represent the average ± SD of three independent experiments.

136x103mm (150 x 150 DPI)

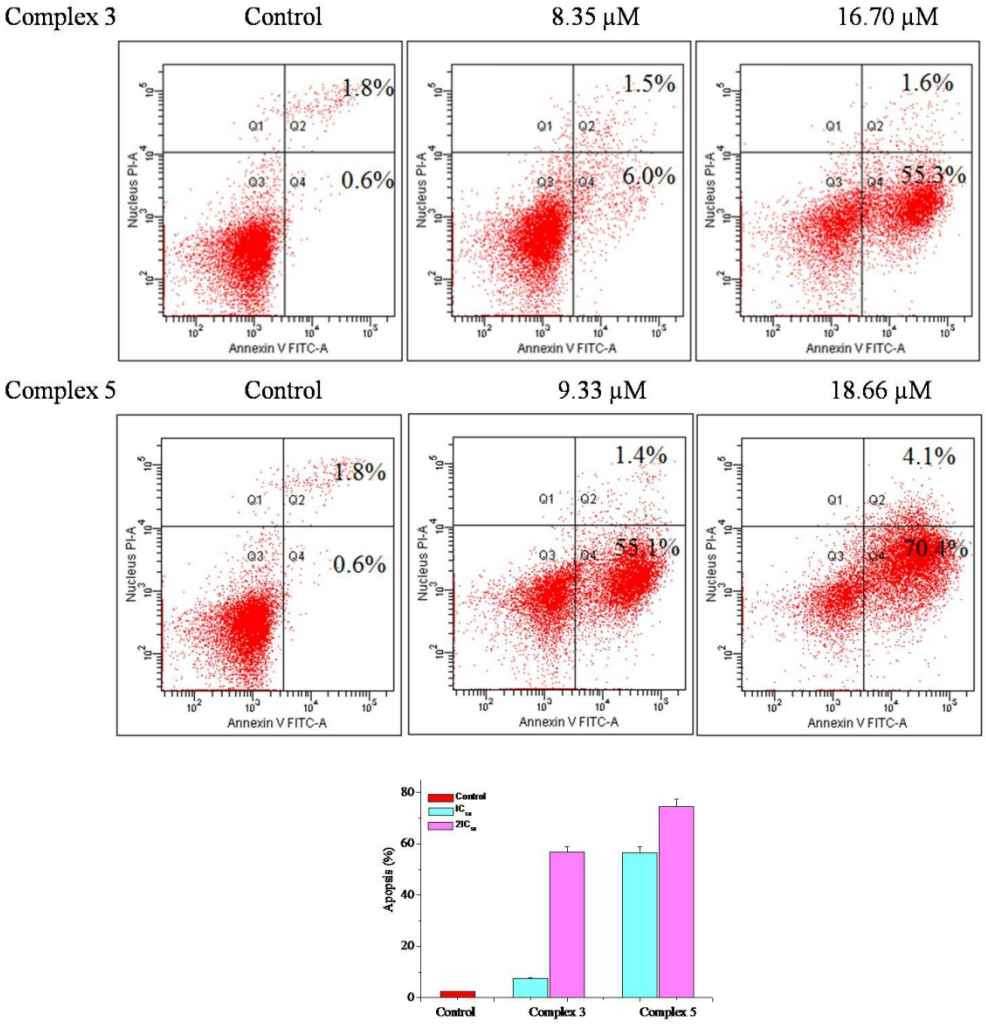

The copper complexes induce apoptosis in TNBC MDA-MB-231 cells. Cells were treated with the copper complexes at 1× and 2 × IC50 concentrations for 24 h and apoptosis detected by flow cytometry using annexin V (x axis)–propidium iodide (y axis) staining. Early apoptotic cells (annexin V-positive, propidium iodide-negative) appear in the lower right quadrant and late apoptotic cells (positive for both markers) in the upper right quadrant. Percentage of cells in apoptotic quadrants is shown. Cytometry plots are representative three independent experiments. Histogram indicates average apoptosis (both early and late) ± SD from three independent experiments.

249x261mm (150 x 150 DPI)

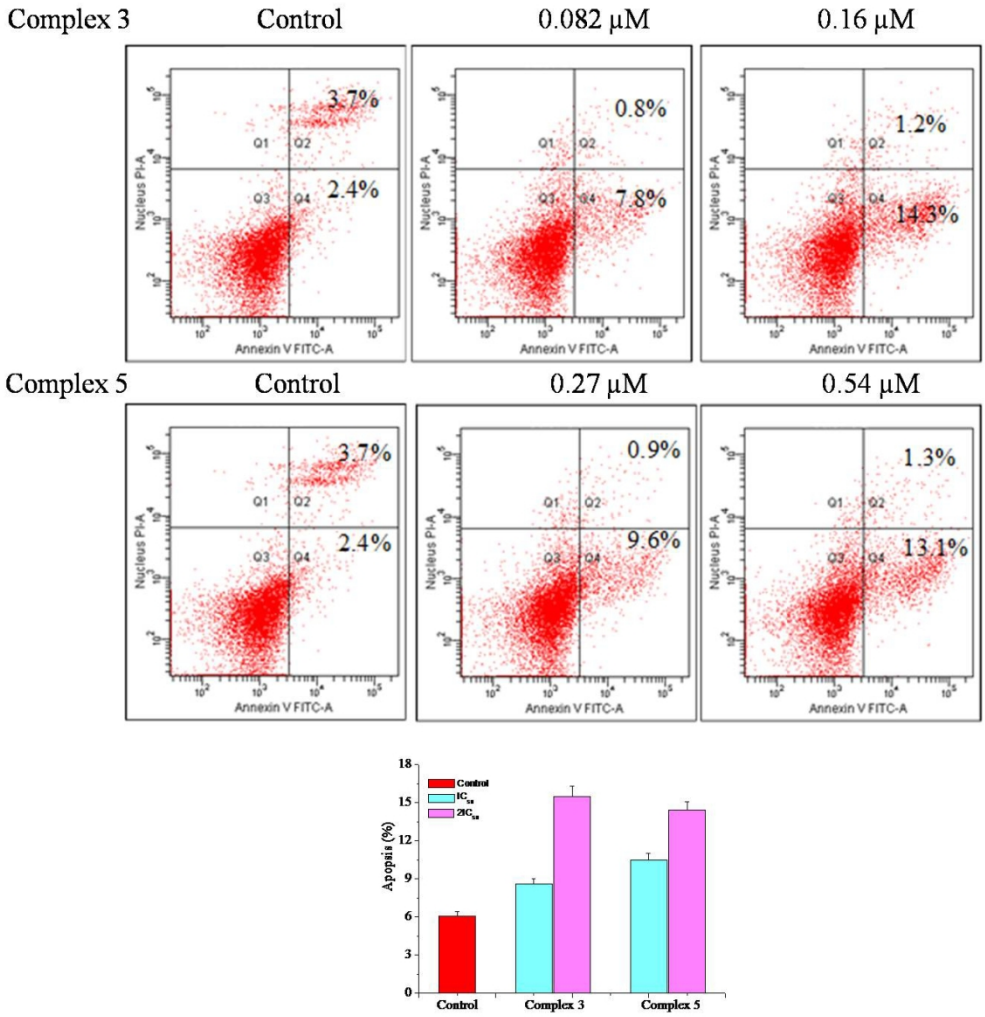

The copper complexes induce apoptosis in TNBC CAL-51 cells. Cells were treated with the copper complexes at 1 × and 2 × IC50 concentrations for 24 h and apoptosis detected by flow cytometry using annexin V (x axis) –propidium iodide (y axis) staining. Early apoptotic cells (annexin V-positive, propidium iodide-negative) appear in the lower right quadrant and late apop-totic cells (positive for both markers) in the upper right quadrant. Percentage of cells in apoptotic quadrants is shown. Cytometry plots are representative three independent experiments. Histogram indicates average apoptosis (both early and late) ± SD from three independent experiments.

226x236mm (150 x 150 DPI)

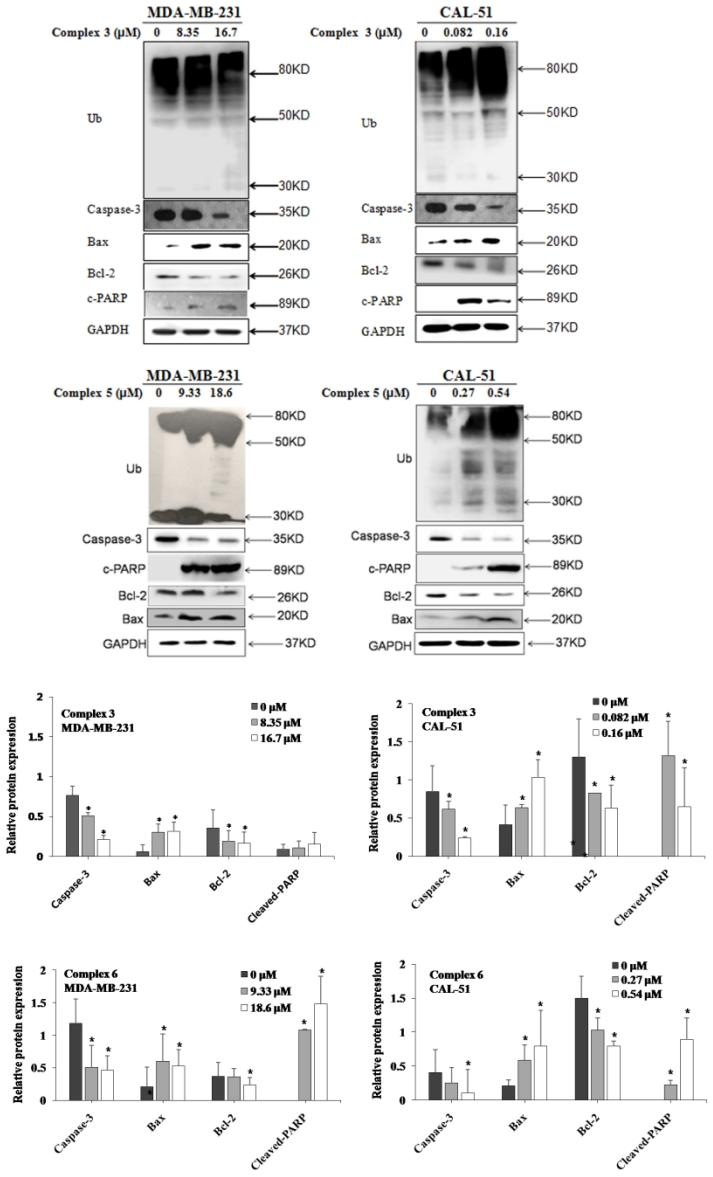

Complexes 3 and 5 induce accumulation of ubiquitinated proteins and apoptosis. Breast cancer MDA-MB-231 and CAL-51 cells were treated with 3 and 5 at 1 × and 2 × IC50 con-centrations for 24 h and ubiquitinated proteins, Caspase-3, PARP, Bcl-2 and Bax. proteins detected by western blotting. House-keeping GAPDH levels were used to confirm equal protein load-ing. Arrow indicates molecular mass in kDa. Band intensity was quantified using Image J and shown as the average ± SD (n=3), *P＜0.05.

290x429mm (150 x 150 DPI)

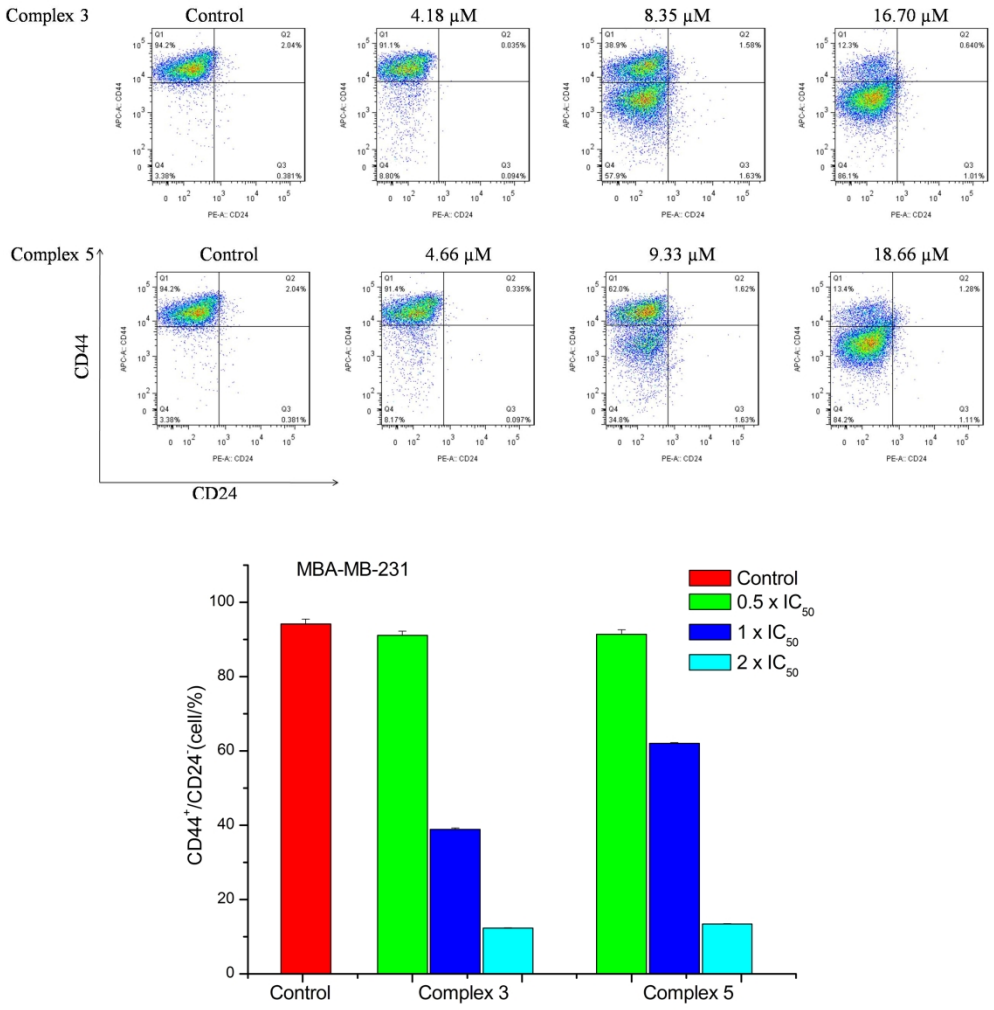

Complexes 3 and 5 decrease stem cell markers in MDA-MB-231 cells. Breast cancer MDA-MB-231 cells were treated with 3 and 5 at 0.5 ×, 1 × and 2 × IC50 concentrations for 24 h and the percentage of the CD44+/CD24- cell subpopulation was determined by flow cytometry. Histogram indicates the average percentage of the CD44+/CD24- cell subpopulation from three independent experiments.

443x494mm (150 x 150 DPI)

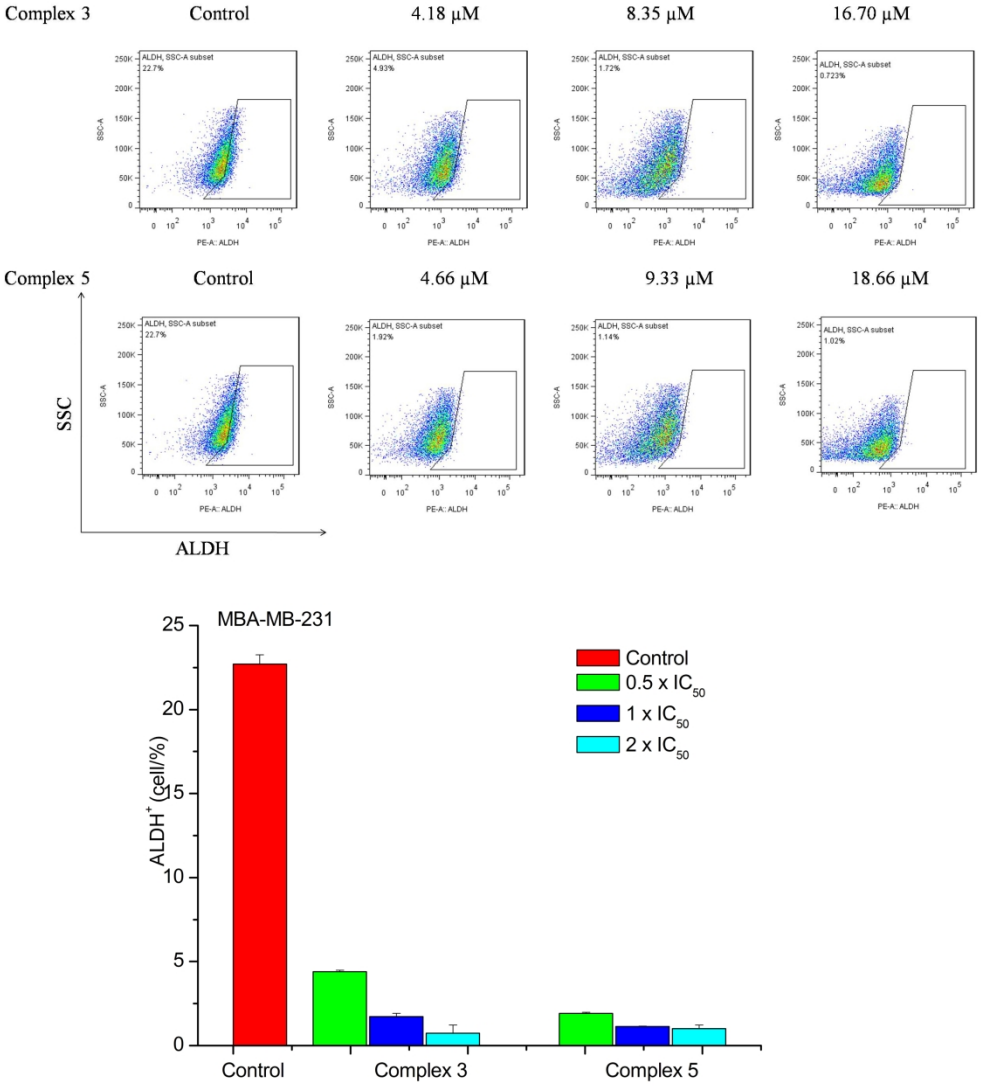

Complexes 3 and 5 decrease stem cell marker ALDH in MDA-MB-231 cells. Breast cancer MDA-MB-231 cells were treated with 3 and 5 at 0.5 ×, 1 × and 2 × IC50 concentrations for 24 h and the percentage of ALDH+ cells determined by flow cytometry. In order to better visualize ALDH+ cells, two-dimensional plots were obtained. SSC, side scatter channel. Histogram indicates the average percentage of the ALDH+ cell subpopulation from three independent experiments.

431x490mm (150 x 150 DPI)

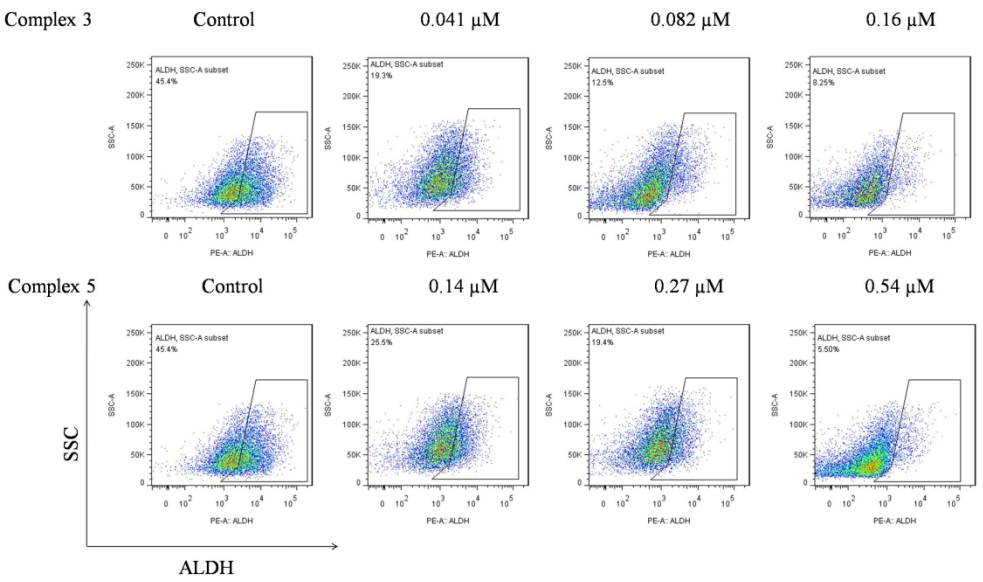

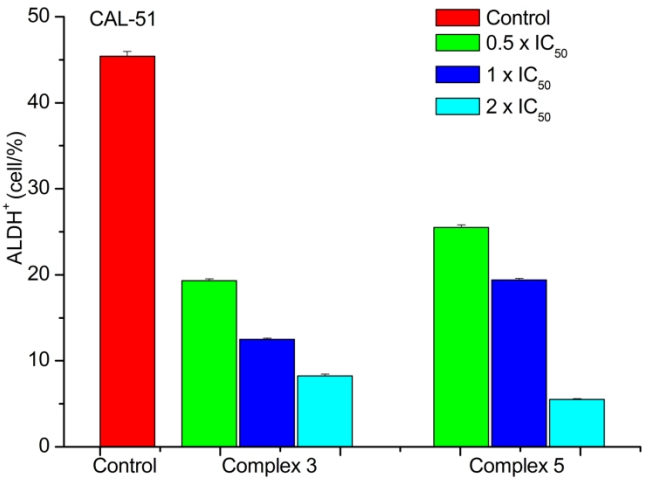

Complexes 3 and 5 decrease stem cell marker ALDH in CAL-51 cells. Breast cancer CAL-51 cells were treated with 3 and 5 at 0.5 ×, 1 × and 2 × IC50 concentrations for 24 h and the per-centage of ALDH+ cells determined by flow cytometry. In order to better visualize ALDH+ cells, two-dimensional plots were obtained. SSC, side scatter channel. Histogram indicates the average percentage of the ALDH+ cell subpopulation from three indepen-dent experiments.

421x490mm (150 x 150 DPI)

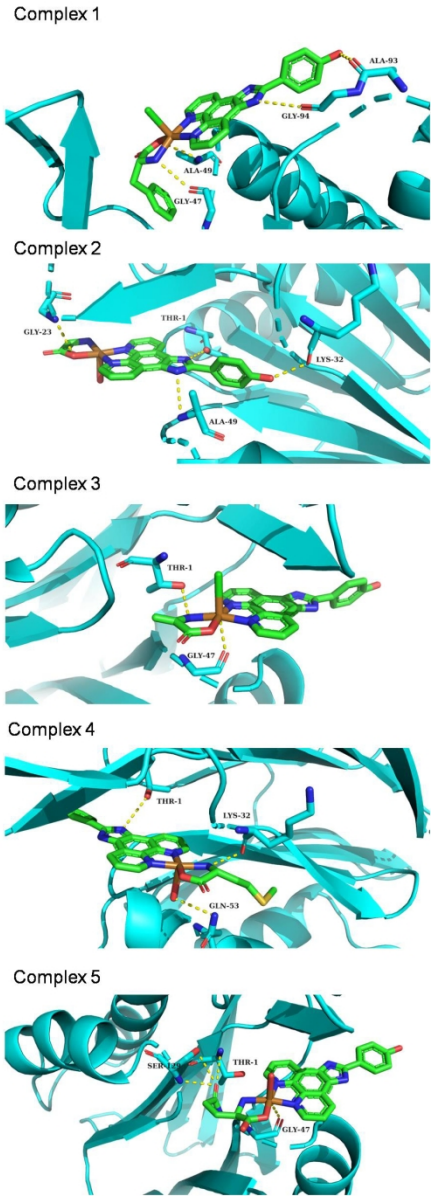

Schematic representation of the proposed binding modes for complexes 1-5 with proteasome (PDB ID:3MG6). Only amino acids located within 4 Å of the bound ligand are displayed and labeled. Key H-bonds between the complexes and the protein are shown as dashed yellow lines.

150x412mm (150 x 150 DPI)

Novel copper complexes that inhibit the proteasome and trigger apoptosis in triple-negative breast cancer cells

Dong-Dong Li [1*], Ernesto Yagüe[3], Lu-Yao Wang[1], Lin-Lin Dai[1], Zi-Bo Yang[1], Shuang Zhi[1], Na Zhang[1], Xiu-Mei Zhao[1*], Yun-Hui Hu[2*]

[1]Tianjin Institute of Medical and Pharmaceutical Sciences, Tianjin 300020, China

[2]The Third Department of Breast Cancer, Tianjin Medical University Cancer Institute and Hospital, Tianjin 300060

[3]Cancer Research Center, Division of Cancer, Faculty of Medicine, Imperial College London, Hammersmith Hospital Campus, London W12 0NN, UK

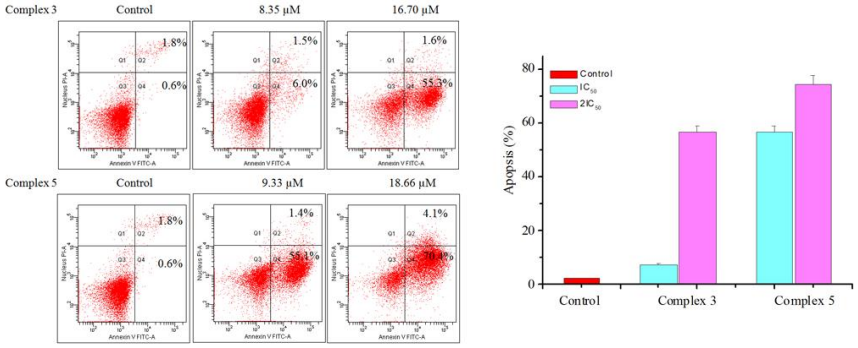

*Corresponding authors:

Dong-Dong Li, Tianjin Institute of Medical and Pharmaceutical Sciences, E-mail address: lidongdong2010@163.com;

Xiu-Mei Zhao, Tianjin Institute of Medical and Pharmaceutical Sciences, E-mail address: zxmmlg@163.com;

Yun-Hui Hu, The Third Department of Breast Cancer, Tianjin Medical University Cancer Institute and Hospital, E-mail: yunhuihu200408@163.com.